Bioorganic & Medicinal Chemistry xxx (2016) xxx–xxx

Contents lists available at ScienceDirect

Bioorganic & Medicinal Chemistry

journal homepage: www.elsevier.com/locate/bmc

Synthesis, biological evaluation and structural analysis of novel peripherally active morphiceptin analogs

Anna Adamska [a], Alicja Kluczyk [b], Maria Camilla Cerlesi [c], Girolamo Calo [c], Anna Janecka [a], Attila Borics [d,*]

[a] Department of Biomolecular Chemistry, Faculty of Medicine, Medical University of Lodz, Mazowiecka 6/8, 92-215 Lodz, Poland
[b] Faculty of Chemistry, University of Wroclaw, F. Joliot-Curie 14, 50-383 Wroclaw, Poland
[c] Department of Medical Sciences, University of Ferrara, Via Fossato di Mortara 17/19, 44121 Ferrara, Italy
[d] Institute of Biochemistry, Biological Research Centre of Hungarian Academy of Sciences, Temesvári krt. 62, Szeged H-6726, Hungary

ARTICLE INFO

Article history:
Received 13 January 2016
Revised 23 February 2016
Accepted 24 February 2016
Available online xxxx

Keywords:
Solid-phase peptide synthesis
Binding studies
Opioid receptors
Hot-plate test
Gastrointestinal transit
Molecular dynamics
Docking

ABSTRACT

Morphiceptin (Tyr-Pro-Phe-Pro-NH_2), a tetrapeptide amide, is a selective ligand of the μ-opioid receptor (MOR). This study reports the synthesis and biological evaluation of a series of novel morphiceptin analogs modified in positions 2 or/and 4 by introduction of 4,4-difluoroproline (F_2Pro) in L or D configuration. Depending on the fluorinated amino acid configuration and its position in the sequence, new analogs behaved as selective full MOR agonists showing high, moderate, or relatively low potency. The most potent analog, Tyr-F_2Pro-Phe-D-F_2Pro-NH_2, was also able to activate the κ-opioid receptor (KOR), although with low potency. Docking studies and the comparison of results with the high resolution crystallographic structure of a MOR-agonist complex revealed possible structure–activity relationships of this compound family.

1. Introduction

A number of milk protein fragments has been shown to behave as opioid receptor ligands, able to address opioidergic systems. One class of such opioid peptides that show some preference for the μ-opioid receptor (MOR)[1,2] is the group of β-casomorphins, originating from the milk protein, β-casein as a product of proteolytic fragmentation. A tetrapeptide amide Tyr-Pro-Phe-Pro-NH_2, known as morphiceptin, shows considerable opioid potency and MOR selectivity.[3] Morphiceptin, among other opioid peptides, elicits strong supraspinal antinociception when given intracerebroventricularly (i.c.v.), in other words directly to the central nervous system (CNS). This effect is not observed after peripheral administration, due to the relatively rapid degradation of morphiceptin, resulting in its short duration of action and limited delivery to the CNS. However, morphiceptin analogs have been proposed as peripheral agents for the treatment of diarrhea. Subcutaneous (s.c.) administration of a potent morphiceptin analog, Tyr-Pro-NMePhe-Pro-NH_2, inhibited diarrhea and decreased gastrointestinal transit in mice.[4] The advantage of such agents is the lack of the central effects, such as analgesia and sedation. Peripheral selectivity of morphiceptin and its analogs encourages further studies of this group of opioid peptides, whose therapeutic possibilities have not been fully appreciated yet.

Morphiceptin was one of the first opioid peptides, of which structure was investigated in detail to explain its affinity to the MOR. The L-configuration of Pro^2 was found vital for manifestation of opioid activity.[5] The phenolic OH and the protonated free amine group of Tyr^1 and the aromatic side chain of Phe^3 in a well-defined relative spatial arrangement were proposed to facilitate high affinity MOR binding, in which pose of the Pro^2 residue acts as a stereochemical spacer responsible for the correct orientation of pharmacophoric groups.[6] However, later studies comparing several MOR ligands of various affinities did not confirm the necessity of an intrinsic tendency of MOR ligands to adopt such spatial arrangement.[7] Instead, many parallel studies revealed that apart from possessing the necessary pharmacophores, the high propensity of a ligand to form bent backbone structure[8–12] or maintain high degree of conformational flexibility[7] may result in high affinity binding to the MOR. In the past, notable emphasis was put on the role of *cis–trans* isomerization of the peptide bond preceding Pro^2 in opioid peptides. As both exclusively *cis*[5] and *trans* peptide ligands[13] were shown to bind to the MOR with high affinity, this structural property was proved to be of little relevance with regard to MOR activity. The X-ray crystallographic structure of both, the

* Corresponding author.
E-mail address: borics.attila@brc.mta.hu (A. Borics).

http://dx.doi.org/10.1016/j.bmc.2016.02.034
0968-0896/

agonist-[14] and antagonist-bound MOR[15] has been published recently, which provided answer to numerous questions regarding ligand structure and activity. Nevertheless, the design of a MOR-agonist peptide with pharmaceutical properties appropriate for therapeutic application remains a challenge.

Unique physico-chemical properties of fluorine, such as small size and high electronegativity, seem to be of special advantage in drug design. Fluorinated compounds show higher bioavailability and metabolic stability. One of the major effects of fluorination is a modulation of acidity of a parent compound which can strongly influence binding affinity and pharmacokinetic properties of an analog. While substitution of fluorine for a hydrogen atom results in minor steric alterations, electrostatic interactions in a molecule may lead to significant conformational changes.[16] So far, only a few fluorinated amino acids have been introduced into the analogs of opioid peptides.[17–19]

In the search for novel morphiceptin analogs with improved pharmacological profile we have synthesized a series of analogs modified in positions 2 or/and 4 by introduction of 4,4-difluoro-Pro (F_2Pro) in L or D configuration (Fig. 1). Novel analogs of morphiceptin were tested in vitro in radioligand receptor binding assays and calcium mobilization-based functional tests. Conformational preferences of the new ligands were studied by performing molecular dynamics (MD) simulations. In order to reveal atomistic details of specific interactions between the new ligands and the MOR, docking studies were performed.

2. Materials and methods

2.1. Peptide synthesis

Most of the chemicals were purchased from Sigma Aldrich. Protected amino acids were purchased from NovaBiochem or Bachem. MBHA Rink-Amide peptide resin (100–200 mesh, 0.6 mmol/g) was obtained from NovaBiochem. Fmoc-protected L- and D-F_2Pro was purchased from TriMen Chemicals (Lodz, Poland). Peptides were synthesized by a standard solid-phase procedure, using technique for Fmoc-protected amino acids on MBHA Rink-Amide resin as described earlier.[20] 20% piperidine in DMF was used for the deprotection of Fmoc groups and TBTU was employed as a coupling

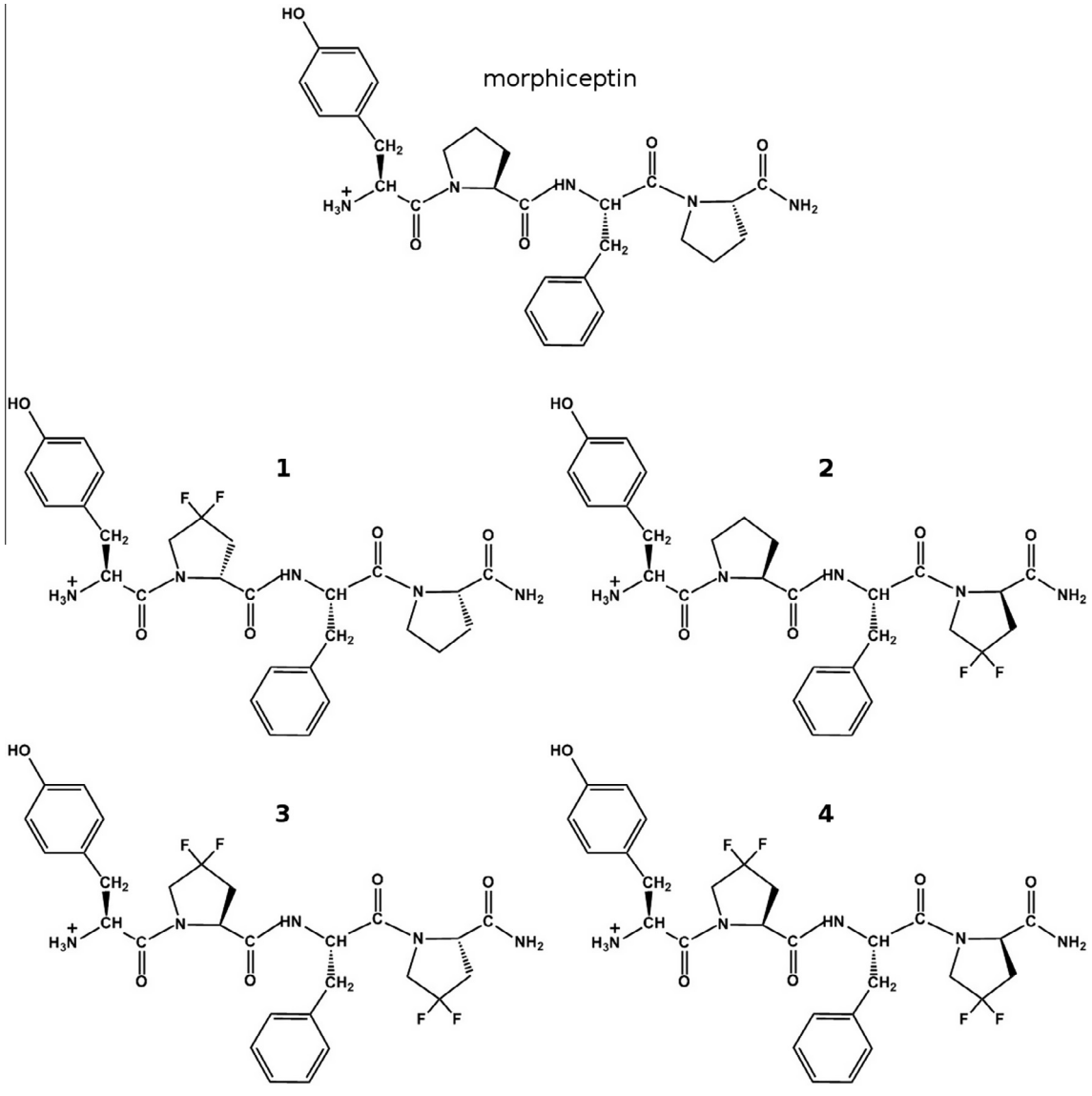

Figure 1. Structure of the studied fluorinated derivatives **1**–**4** and their parent compound, morphiceptin.

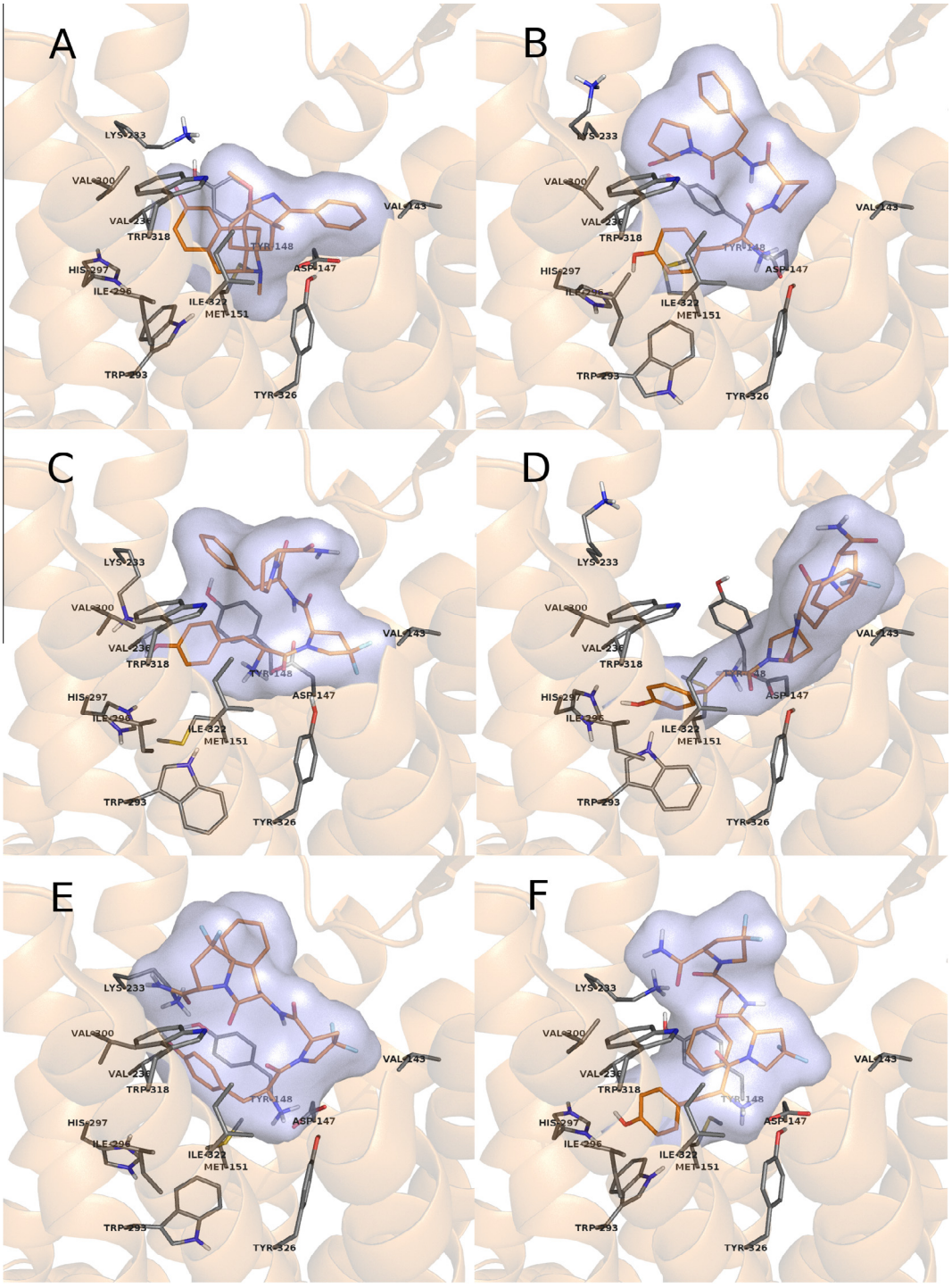

Figure 2. Specifically bound, low energy docked complexes of morphiceptin (B), **1** (C), **2** (D), **3** (E) and **4** (F) in comparison with the crystallographic structure of a MOR-bound morphinan agonist BU42 (A).

agent. Simultaneous deprotection and cleavage from the resin was accomplished by treatment with TFA/TIS/water (95:2.5:2.5) for 3 h at room temperature.

Crude peptides were purified by preparative RP-HPLC on a Vydac C_{18} column (10 μm, 22 × 250 mm) equipped with a Vydac guard cartridge. The solvent system of 0.1% TFA in water (A)/80% acetonitrile in water containing 0.1% TFA (B) and a linear gradient of 0–100% B over 15 min was used. The purity of the final peptides was verified by analytical HPLC employing a Vydac C_{18} column (5 μm, 4.6 × 250 mm) and the solvent system of 0.1% TFA in water (A)/80% acetonitrile in water containing 0.1% TFA (B). A linear gradient of 0–100% B over 50 min at a flow rate of 1 ml/min was used for the analysis. Identity of the synthesized peptides was characterized by high resolution mass spectroscopy, using Bruker micrOTOF-Q mass spectrometer (Bruker Daltonics, Bremen, Germany) with electrospray ionization (ESI-MS).

2.2. Receptor binding assays

Receptor binding assays were performed according to the modified method described by Misicka et al.,[21] using brain homogenates of adult male Wistar rats (for MOR and δ-opioid receptor,

DOR) or adult male Dunkin Hartley guinea pigs (for κ-opioid receptor, KOR). The opioid receptor binding affinities for MOR, DOR and KOR were determined by radioligand competition analysis using [^{3}H]DAMGO, [^{3}H][Ile^{5,6}]deltorphin-2 and [^{3}H]nor-BNI, respectively. Three independent experiments for each assay were carried out in duplicate. The data were analyzed by a nonlinear least square regression analysis computer program Graph Pad PRISM 6.0 (Graph Pad Software Inc., San Diego, USA).

2.3. Calcium mobilization assay

Chinese Hamster Ovary (CHO) cells stably co-expressing human recombinant MOR or KOR and the C-terminally modified $G\alpha_{qi5}$ and CHO cells co-expressing the human recombinant DOR receptor and the $G\alpha_{qG66Di5}$ chimeric protein were generated as previously described.[22–24]

Agonist potencies were given as pEC_{50} representing a negative logarithm of the molar concentration of an agonist that produces 50% of the maximal possible effect. Concentration response curves were fitted with the four parameter logistic nonlinear regression model:

$$\text{Effect} = \text{baseline} + \frac{E_{max} - \text{baseline}}{1 + 10^{(\log EC_{50} - X)\cdot n}}$$

where X is the agonist concentration and n is the Hill coefficient. Ligand efficacy was expressed as intrinsic activity (α) calculated as the E_{max} of the ligand to E_{max} of the standard agonist ratio. Curve fittings were performed using GraphPad PRISM 6.0 (GraphPad Software Inc., San Diego, USA).

2.4. MD simulations

MD simulations of compounds **1**–**4** were started from extended, energy minimized geometries and executed using the GROMACS 5.0.4 program package and the AMBER ff03 force field parameter set.[25] Parameters for unnatural amino acid residues were supplemented from the generalized Amber force field (gAFF)[26] and partial charges were determined at the HF/6-31G(d) level using the restrained electrostatic potential (RESP) method with the same force field parameters as described above. Each starting structure was immersed in a cubic box (35 Å × 35 Å × 35 Å) of pre-equilibrated TIP3P[27] water molecules. Solvent molecules were removed from the box when the distance between any atom of the solute and solvent molecules was less than the sum of their van der Waals radii. Protonated N-termini of peptides were neutralized by replacing solvent molecules by Cl-ions at a position with the most favorable electrostatic potential. All systems were then subjected to 1000 steps of steepest descent, followed by 1000 steps conjugate gradient energy minimization with 0.001 kJ mol^{-1} convergence criteria. In order to allow the solvent density to equilibrate, 0.5 ns NVT MD simulations at 300 K were performed while the position of the solute was fixed in the center of the box with a force constant of 1000 kJ mol^{-1} Å^2 on each heavy atom. Subsequently, 200.5 ns NPT MD simulations were performed for the four peptides, each at constant temperature (300 K) and pressure (1 bar), with the following parameters: the time step was set to 2 fs, the LINCS algorithm was used to constrain all bonds to their correct lengths, temperature was regulated with the v-rescale algorithm with a coupling constant of 0.1 ps, constant pressure was maintained using isotropic scaling with a relaxation constant of 1.0 ps and 4.5×10^{-5} bar^{-1} isothermal compressibility. Non-bonded interactions were calculated using the PME method with all cut-off values set at 12 Å. The coordinates were stored after every 1000 steps to yield a total of 100,000 sampled conformations for each trajectory, after excluding the first 0.5 ns of equilibration.

The evolution of secondary structure of the peptides along each trajectory was analyzed with the STRIDE algorithm[28] and Perl scripts written in-house. The analysis programs of the GROMACS 5.0.4 program suite was used for the measurement of the C(1)–C_α(2)–C_α(3)–N(4) virtual dihedral angle and the distance between the terminal C_α atoms. A bend structure was assigned when this dihedral angle was between −80° and 80° and the distance was less than 10.0 Å.[29]

2.5. Docking studies

The crystallographic structure of the active murine MOR (PDB code: 5C1M)[13] was used as docking target after missing side chains were added. Dockings were performed with the Autodock 4.2 software. Side chains in contact with the bound ligand, observed in the crystal complex of MOR and BU72 were kept flexible as well as all Φ, ψ and χ^1 ligand torsions. Blind docking of morphiceptin and derivatives **1**–**4** were performed using the Lamarckian genetic algorithm in a 80 Å × 80 Å × 80 Å grid volume, large enough to cover the whole receptor region accessible from the extracellular side. The spacing of grid points was set at 0.375 Å and 1000 dockings were done for all ligands. The resultant ligand–receptor complexes were clustered and ranked according to the corresponding binding free energies. In silico inhibitory constants were calculated according to the following equation: $\Delta G = RT \ln K_i$. The pool of ligand–receptor complexes was reduced by excluding the bound states in which specific, conserved ligand–receptor interactions observed in the crystallographic structures of the MOR complexes[14,15] were not present.

3. Results and discussion

3.1. Peptide synthesis

Peptides were synthesized by the conventional solid-phase procedure on the MBHA Rink Amide resin, using techniques for Fmoc-protected amino acids. High resolution mass spectrometry (ESI-MS) confirmed the identity of all synthesized peptides (see Supplementary material). RP-HPLC analyses of the final purified products indicated purity of 97% or greater (Table 1).

3.2. Opioid receptor binding studies

Opioid receptor binding affinities of peptides for the MOR, DOR and KOR were determined by radioligand competition analysis using [^{3}H]DAMGO, [^{3}H][Ile^{5,6}]deltorphin-2 and [^{3}H]nor-BNI, respectively. The IC_{50} values were determined from logarithmic dose–displacement curves, and the values of the inhibitory

Table 1
Physicochemical data of new opioid peptide analogs

No.	Sequence	Formula	m/z [M+H]$^+$[a]		HPLC t_R[b] (min)
			Calcd	Obsd	
1	Tyr-D-F_2Pro-Phe-Pro-NH_2	$C_{28}H_{34}F_2N_5O_5$	558.252	558.252	14.10
2	Tyr-Pro-Phe-D-F_2Pro-NH_2	$C_{28}H_{34}F_2N_5O_5$	558.252	558.271	14.22
3	Tyr-F_2Pro-Phe-F_2Pro-NH_2	$C_{28}H_{32}F_4N_5O_5$	594.233	594.244	14.56
4	Tyr-F_2Pro-Phe-D-F_2Pro-NH_2	$C_{28}H_{32}F_4N_5O_5$	594.233	594.247	14.99

[a] Mass was measured using ESI-MS.
[b] t_R with Vydac C_{18} column (5 μm, 4.6 × 250 mm) using the solvent system of 0.1% TFA in water (A) and 80% acetonitrile in water containing 0.1% TFA (B) and a linear gradient of 0–100% solvent B over 50 min, with the flow rate 1 ml/min.

constant (K_i) of peptides were calculated according to the equation of Cheng and Prusoff[30] are shown in Table 2. Morphiceptin, as expected, displayed only mild affinity for MOR but high selectivity for this receptor. Among the new analogs, only **2** and **4** with D-configured F_2Pro in position 4 were able to bind to MOR. Analog **4**, with two fluorinated Pro residues (L, D, respectively) showed subnanomolar affinity for MOR and very weak for KOR, although considering that [^{3}H]nor-BNI is also very weak MOR ligand, the measured KOR affinity may be argued at this point. As compared to the earlier described analog, Tyr-Pro-Phe-D-Pro-NH_2 (IC_{50} = 4.3 nM),[31] it seems that fluorination increased MOR affinity by an order of magnitude.

3.3. Functional assay

The pharmacological profiles of peptides were characterized in vitro at all three opioid receptors in calcium mobilization assays.[24] The calculated agonist potencies (pEC_{50}) and efficacies (α) of the analogs are summarized in Table 3. Dermorphin, DPDPE, and dynorphin A were used as the reference agonists for calculating intrinsic activity at the MOR, DOR, and KOR, respectively.

Results of this study demonstrated that all novel compounds behaved as selective full agonists of MOR showing high (**4**), moderate (**2**), or relatively low (**3**) potency. Compound **4** is also able to activate the KOR with low potency (MOR/KOR selectivity 174 fold), which suggests that the measured low KOR binding affinity of this analog is not an artifact emerging from the applied experimental conditions.

3.4. MD simulations

MD simulations were performed to investigate the relationship between the MOR binding properties and conformational preferences of compounds **1**–**4**. Results of trajectory analysis are summarized in Table 4. All morphiceptin analogs were found to adopt various γ and β-turns with similar frequency as it was observed for the parent compound morphiceptin in a previous study.[7] As a result of a tertiary amide in position 4 of the sequences, no β-turn types stabilized through a $1 \leftarrow 4$ hydrogen bond were found. Neither any of the identified specific secondary structural elements, nor their population were found to correlate with MOR affinity. The tendency of compounds **1**–**4** to form bent backbone structure, which was indicated previously to be advantageous for MOR binding was found to be significantly lower than that of the parent compound. However, it was also reported earlier that ligands which are not likely to form bent structure in solution, but maintain considerable conformational flexibility, such as DAMGO, the prototypical ligand of the MOR, can still bind to the receptor with high affinity.[7] In summary, conformational preferences of these ligands, determined in the absence of the receptor do not rule out the possibility of high affinity binding and receptor activation, but on the other hand do not provide basis for the explanation of in vitro experimental results.

3.5. Docking studies

Configuration inversion and/or fluorination of the Pro residues in morphiceptin in this study were disproved to result in such a significant change of conformational preferences that could be held responsible for the observed differences in bioactivity. In order to gain explanation, the aim was set to study the specific interactions formed by the receptor bound ligands. Dockings of morphiceptin and compounds **1**–**4** were performed to investigate how configuration inversion and fluorination of the Pro residues of morphiceptin affect interactions with the MOR. It is known for most docking algorithms that they may present low energy bound structures even for compounds which do not show any affinity for the receptor in experiments.[32] Such occurrence of false positive hits is usually even higher in the case of ligands with high conformational flexibility.

Blind, flexible docking of morphiceptin and analogs **1**–**4** to the MOR resulted in low energy complexes in which all the ligands were located in the previously described binding cavity. The K_i values calculated for the lowest binding free energy complexes suggest high affinity binding of these ligands in general (Table 2). However, the relative receptor–ligand orientation in the bound ligands did not reflect any structural specificity. In order to exclude the non-specifically bound ligand conformations from analysis, the low energy ligand–receptor complexes were inspected for the presence of previously described interactions. A salt bridge between the positively charged amino groups of opioid ligands and Asp^{147} of the mouse MOR was shown to be essential both by structure–activity studies[10] and site-directed mutagenesis of the receptor.[33] The presence of this interaction was confirmed in the crystallographic complexes.[14,15] Furthermore, the tertiary amine group and the phenolic OH group of the MOR bound morphinan agonist BU72 were found to adopt an alignment identical to that of the MOR bound morphinan antagonist β-FNA, suggesting that regardless of functional properties of ligands, this structural arrangement is a requisite of high affinity binding. The above mentioned functional groups of morphinan ligands are analogous to the phenolic OH and free amine pharmacophores of Tyr^1 in opioid peptides. Consequently, docked ligand–receptor complexes in which the conserved salt bridge and correct alignment of pharmacophores were not present, including some of the lowest energy ones, were considered as non-specifically bound and excluded from further analysis.

Lowest binding free energy complexes of the specifically bound fluorinated analogs **1**–**4** and their parent compound, in comparison

Table 2
In vitro and in silico opioid receptor binding data of fluorinated morphiceptin analogs

No.	Sequence	K_i[a] (nM)			In silico K_i[b] (nM)	
		MOR	DOR	KOR	MOR non-specific[c]	MOR specific[d]
	Tyr-Pro-Phe-Pro-NH_2 (morphiceptin)	36.39	>1000	>1000	0.72	21.44
1	Tyr-D-F_2Pro-Phe-Pro-NH_2	>1000	>1000	>1000	1.99	121.35
2	Tyr-Pro-Phe-D-F_2Pro-NH_2	13.28	>1000	>1000	0.48	35.91
3	Tyr-F_2Pro-Phe-F_2Pro-NH_2	105.63	>1000	>1000	1.52	103.18
4	Tyr-F_2Pro-Phe-D-F_2Pro-NH_2	0.37	>1000	385.90	0.81	1.73

[a] Binding affinity values determined by competitive displacement of the selective radioligands, [^{3}H]DAMGO (for MOR) and [^{3}H][Ile^{5,6}]deltorphin-2 (for DOR), using rat brain membranes, and [^{3}H]nor-BNI (for KOR) using guinea pig brain membranes.
[b] Theoretical inhibitory constants were calculated from binding free energies resulting from docking studies using the following equation: $\Delta G = RT \ln K_i$.
[c] Overall lowest binding free energy complexes.
[d] Lowest binding free energy complexes which possess the conserved receptor–ligand interactions.

Please cite this article in press as: Adamska, A.; et al. *Bioorg. Med. Chem.* (2016), http://dx.doi.org/10.1016/j.bmc.2016.02.034

Table 3
Effects of reference agonists and compounds assessed at human recombinant opioid receptors coupled with calcium signaling via chimeric G proteins

Compound	MOR		DOR		KOR	
	pEC_{50} ($CL_{95\%}$)	α ± SEM	pEC_{50} ($CL_{95\%}$)	α ± SEM	pEC_{50} ($CL_{95\%}$)	α ± SEM
Dermorphin	8.40 (8.12–8.68)	1.00	6.43 (5.95–6.91)	1.03 ± 0.07[a]	Inactive[a]	
DPDPE	Inactive[a]		7.77 (7.38–8.16)	1.00	Inactive[a]	
Dynorphin A	6.67 (6.17–7.17)	0.83 ± 0.10[a]	7.73 (7.46–8.00)	0.99 ± 0.04[a]	8.82 (8.62–9.02)	1.00
Morphiceptin	6.13 (5.86–6.39)	0.96 ± 0.04	Inactive		Inactive	
1	Inactive		Inactive		Inactive	
2	7.69 (7.41–7.97)	1.06 ± 0.11	Inactive		Crc incomplete	
3	6.40 (6.15–6.66)	1.03 ± 0.08	Inactive		Inactive	
4	8.33 (8.03–8.64)	1.04 ± 0.06	Inactive		6.09 (5.92–6.27)	0.84 ± 0.06*

Inactive means that the compound was inactive up to 1 μM.
Crc incomplete means that maximal effects could not be determined due to the low potency of the compounds. Dermorphin, DPDPE and dynorphin A were used as reference agonists for calculating intrinsic activity at MOR, DOR, and KOR receptor, respectively.
[a] These data are from Camarda and Calò.[24]
* $p < 0.05$ according to one way ANOVA followed by the Dunnett's test for multiple comparisons.

Table 4
Frequency of canonical secondary structural elements identified by STRIDE analysis and the overall occurrence of bent backbone structure

Secondary structural element	Residues involved	Population[a] (%)			
		1	**2**	**3**	**4**
Type IV β-turn	Tyr^1-Pro^4/F_2Pro^4	1.63	3.59	1.75	1.89
Type VIII β-turn	Tyr^1-Pro^4/F_2Pro^4	—	3.62	1.96	3.59
Inverse γ-turn	Tyr^1-Phe^3	—	10.08	12.85	16.05
Inverse γ-turn	Phe^3-Pro^4/F_2Pro^4-NH_2	5.39	—	7.01	—
Classic γ-turn	Phe^3-Pro^4/F_2Pro^4-NH_2	—	2.58	—	1.60
Inverse γ-turns	Tyr^1-Phe^3, Phe^3-Pro^4/F_2Pro^4-NH_2	—	—	1.39	—
Inverse + classic γ-turns	Tyr^1-Phe^3, Phe^3-Pro^4/F_2Pro^4-NH_2	—	—	—	0.44
Bend structure[b]	Any possible	8.73	8.12	4.85	6.86

[a] Population fraction of the total conformational ensemble generated by MD simulations.
[b] Bent structure was assigned based on the analysis of the N(1)–C_α(2)–C_α(3)–C(4) virtual dihedral angle and the distance between the terminal C_α-atoms.

to the crystallographic structure of a MOR-bound morphinan agonist are shown in Figure 2. Theoretical K_i values calculated for these complexes fairly reproduce the experimentally observed values and their differences, providing basis for structural explanation of receptor affinity. In general, *trans* conformation of the Tyr^1 side chain was found to furnish the desired alignment of pharmacophores described above and apart from one exception (Fig. 2D), ligands were found to bind in a bent backbone structure (Fig. 2). This observation confirms hypotheses included in previous pharmacophore models.[10] Pro^2 and F_2Pro^2 of the studied compounds were observed to occupy the same, mainly hydrophobic cavity formed by residues Trp^{133}, Val^{143} and Ile^{144}, as the pendant phenyl group of BU72 in the crystal structure of the active MOR. This suggests, that fluorination of Pro^2 may give rise to the strength of hydrophobic interactions between the ligand and the receptor. Furthermore, it gives explanation for lower receptor affinities observed for endomorphin analogs with hydroxyproline substitution in this position of the sequence.[34,35] The D configuration of F_2Pro^2 in **1** was shown to have a deleterious effect on receptor binding which is also in agreement with previous observations.[5,36] However, inspecting receptor–ligand complexes in Figure 2 it is apparent that Pro^2/F_2Pro^2 could interact with the same hydrophobic side chains of the binding cavity in both L and D configuration. Apparently, the LDLL configuration pattern of compound **1** results in the projection of the hydrophobic Phe^3 side chain into the pocket region lined by Tyr^{148}, Lys^{233} and His^{297} (Fig. 2C) and disrupting the water molecule assisted polar network essential for the proper function of the receptor.[14,37] Analog **1** is unique in this sense among the studied compounds as morphiceptin and analogs **2–4** were more likely to leave this polar network intact (Fig. 2D) or extend it by contributing their C-terminal amide group (Fig. 2BEF). D configuration of Pro^4/F_2Pro^4 may provide a further advantage in this model by placing the apolar Pro^4/F_2Pro^4 side chain away from the polar network (Fig. 2F).

4. Conclusion

Substitution of the Pro^2 and Pro^4 residues of morphiceptin by L- and/or D-F_2Pro resulted in a series of analogs with diverse bioactivity a new, high affinity MOR-selective peptide ligand **4** was presented. The solution conformational preferences of these compounds in aqueous media were found to be highly similar, suggesting that the observed differences in MOR affinity may be attributed to different ligand receptor contacts and specific interactions rather than conformational selection. The recently published high resolution structure of the active and inactive MOR proved to be a solid independent platform for the evaluation of receptor bound geometries of peptide ligands obtained from docking. Using these structures as a reference facilitated the explanation of the structure–activity relationships of the studied compounds. Previous suggestions for the MOR-bound ligand structure such as bent backbone and *trans* conformation of the Tyr^1 side chain were confirmed. In addition to the well described interactions with the conserved Asp^{147} and the polar network formed by Tyr^{148}, Lys^{233} and His^{297} of the receptor, Pro^2 and F_2Pro^2 of the studied compounds were found to locate in a cavity of hydrophobic character, lined by residues Trp^{133}, Val^{143} and Ile^{144}. Substitution of Pro^2 to the more hydrophobic derivative F_2Pro^2 appears to be beneficial for the formation of stronger ligand–receptor interactions. In general, our results indicate that observations of specific MOR–ligand interactions in experimental and in silico complex models could constitute the basis of the future design of MOR ligands with fine-tuned chemical structure and optimal effectiveness.

Acknowledgements

This work was supported by Hungarian-Polish Non-Governmental Cooperation Programme. Research of A.B. has been supported by the János Bolyai Research Scholarship of the Hungarian Academy of Sciences.

Supplementary data

Supplementary data associated with this article can be found, in the online version, at http://dx.doi.org/10.1016/j.bmc.2016.02.034.

References and notes

1. Andresen, V.; Camilleri, M. *Drugs* **2006**, *66*, 1073.
2. Arhan, P.; Devroede, G.; Jehannin, B.; Lanza, M.; Faverdin, C.; Dornic, C.; Persoz, B.; Tétreault, L.; Perey, B.; Pellerin, D. *Dis. Colon Rectum.* **1981**, *24*, 625.
3. Janecka, A.; Fichna, J.; Mirowski, M.; Janecki, T. *Mini Rev. Med. Chem.* **2002**, *2*, 565.
4. Shook, J. E.; Lemcke, P. K.; Gehrig, C. A.; Hruby, V. J.; Burks, T. F. *J. Pharmacol. Exp. Ther.* **1989**, *249*, 83.
5. Keller, M.; Boissard, C.; Patiny, L.; Chung, N. N.; Lemieux, C.; Mutter, M.; Schiller, P. W. *J. Med. Chem.* **2001**, *44*, 3896.
6. Yamazaki, T.; Ro, S.; Goodman, M.; Chung, N. N.; Schiller, P. W. *J. Med. Chem.* **1993**, *36*, 708.
7. Borics, A.; Tóth, G. *J. Mol. Graphics Modell.* **2010**, *28*, 495.
8. Eguchi, M.; Shen, R. Y. W.; Shea, J. P.; Lee, M. S.; Kahn, M. *J. Med. Chem.* **2002**, *45*, 1395.
9. Tömböly, C.; Ballet, S.; Feytens, D.; Kövér, K. E.; Borics, A.; Lovas, S.; Al-Khrasani, M.; Fürst, Z.; Tóth, G.; Benyhe, S.; Tourwé, D. *J. Med. Chem.* **2008**, *51*, 173.
10. Keresztes, A.; Borics, A.; Tóth, G. *ChemMedChem* **2010**, *5*, 1176.
11. Gentilucci, L.; Tolomelli, A.; De Marco, R.; Spampinato, S.; Bedini, A.; Artali, R. *ChemMedChem* **2011**, *6*, 1640.
12. Piekielna, J.; Gentilucci, L.; De Marco, R.; Perlikowska, R.; Adamska, A.; Olczak, J.; Mazur, M.; Artali, R.; Modranka, J.; Janecki, T.; Tömböly, C.; Janecka, A. *Bioorg. Med. Chem.* **2014**, *22*, 6545.
13. Keresztes, A.; Szűcs, M.; Borics, A.; Kövér, K. E.; Forró, E.; Fülöp, F.; Tömböly, C.; Péter, A.; Páhi, A.; Fábián, G.; Murányi, M.; Tóth, G. *J. Med. Chem.* **2008**, *51*, 4270.
14. Huang, W.; Manglik, A.; Venkatakhrisnan, A. J.; Laeremans, T.; Feinberg, E. N.; Sanborn, A. L.; Kato, H. E.; Livingston, K. E.; Thorsen, T. S.; Kling, R. C.; Granier, S.; Gmeiner, P.; Husbands, S. M.; Traynor, J. R.; Weis, W. I.; Steyaert, J.; Dror, R. O.; Kobilka, B. K. *Nature* **2015**, *524*, 315.
15. Manglik, A.; Kruse, A. C.; Kobilka, T. S.; Thian, F. S.; Mathiesen, J. M.; Sunahara, R. K.; Pardo, L.; Weis, W. I.; Kobilka, B. K.; Granier, S. *Nature* **2012**, *485*, 321.
16. Wang, J.; Sánchez-Roselló, M.; Aceña, J. L.; del Pozo, C.; Sorochinsky, A. E.; Fustero, S.; Soloshonok, V. A.; Liu, H. *Chem. Rev.* **2014**, *114*, 2432.
17. Honda, T.; Shirasu, N.; Isozaki, K.; Kawano, M.; Shigehiro, D.; Chuman, Y.; Fujita, T.; Nose, T.; Shimohigashi, Y. *Bioorg. Med. Chem.* **2007**, *15*, 3883.
18. Mallareddy, J. R.; Borics, A.; Keresztes, A.; Kövér, K. E.; Tourwé, D.; Tóth, G. *J. Med. Chem.* **2011**, *54*, 1462.
19. De Marco, R.; Andrea Bedini, A.; Spampinato, S.; Gentilucci, L. *J. Med. Chem.* **2014**, *57*, 6861.
20. Adamska, A.; Kolesińska, B.; Kluczyk, A.; Kamiński, Z. J.; Janecka, A. *J. Pept. Sci.* **2015**, *21*, 807.
21. Misicka, A.; Lipkowski, A. W.; Horvath, R.; Davis, P.; Kramer, T. H.; Yamamura, H. I.; Hruby, V. J. *Life Sci.* **1992**, *51*, 1025.
22. Conklin, B. R.; Farfel, Z.; Lustig, K. D.; Julius, D.; Bourne, H. R. *Nature* **1993**, *363*, 274.
23. Kostenis, E.; Martini, L.; Ellis, J.; Waldhoer, M.; Heydorn, A.; Rosenkilde, M. M.; Norregaard, P. K.; Jorgensen, R.; Whistler, J. L.; Milligan, G. *J. Pharmacol. Exp. Ther.* **2005**, *313*, 78.
24. Camarda, V.; Calo', G. *Methods Mol. Biol.* **2013**, *937*, 293.
25. Duan, Y.; Wu, C.; Chowdhury, S.; Lee, M. C.; Xiong, G. M.; Zhang, W.; Yang, R.; Cieplak, P.; Luo, R.; Lee, T.; Caldwell, J.; Wang, J. M.; Kollman, P. *J. Comput. Chem.* **2003**, *24*, 1999.
26. Wang, J.; Wolf, R. M.; Caldwell, J. W.; Kollman, P. A. *J. Comput. Chem.* **2004**, *25*, 1157.
27. Jorgensen, W. L.; Chandrasekhar, J.; Madura, J.; Klein, M. L. *J. Chem. Phys.* **1983**, *79*, 926.
28. Frishman, D.; Argos, P. *Proteins* **1995**, *23*, 566.
29. Ball, J. B.; Hughes, R. A.; Alewood, P. F.; Andrews, P. R. *Tetrahedron* **1993**, *49*, 3467.
30. Cheng, Y. C.; Prusoff, W. H. *Biochem. Pharmacol.* **1973**, *22*, 3099.
31. Chang, K. J.; Wei, E. T.; Killian, A.; Chang, J. K. *J. Pharmacol. Exp. Ther.* **1983**, *227*, 403.
32. Feig, M.; Onufriev, A.; Lee, M. S.; Im, W.; Case, D. A.; Brooks, C. L. *J. Comput. Chem.* **2004**, *25*, 265.
33. Surratt, C. K.; Johnson, P. S.; Moriwaki, A.; Seidleck, B. K.; Blaschak, C. J.; Wang, J. B.; Uhl, G. R. *J. Biol. Chem.* **1994**, *269*, 20548.
34. Biondi, B.; Giannini, E.; Negri, L.; Melchiorri, P.; Lattanzi, R.; Rosso, F.; Ciocca, L.; Rocchi, R. *Int. J. Pept. Res. Ther.* **2006**, *12*, 145.
35. Borics, A.; Mallareddy, J. R.; Timári, I.; Kövér, K. E.; Keresztes, A.; Tóth, G. *J. Med. Chem.* **2012**, *55*, 8418.
36. Giordano, C.; Sansone, A.; Masi, A.; Lucente, G.; Punzi, P.; Mollica, A.; Pinnen, F.; Feliciani, F.; Cacciatore, I.; Davis, P.; Lai, J.; Ma, S. W.; Porreca, F.; Hruby, V. J. *Eur. J. Med. Chem.* **2010**, *45*, 4594.
37. Sounier, R.; Mas, C.; Steyaert, J.; Laeremans, T.; Manglik, A.; Huang, W.; Kobilka, B. K.; Déméné, H.; Granier, S. *Nature* **2015**, *524*, 375.

Please cite this article in press as: Adamska, A.; et al. *Bioorg. Med. Chem.* (2016), http://dx.doi.org/10.1016/j.bmc.2016.02.034